Evolutionary algorithm simulation study of β-MnO₂ nanoclusters

P W Masoga, P E Ngoepe and R R Maphanga

Materials Modelling Centre, School of Physical and Mineral Sciences, University of Limpopo, Private bag x 1106, Sovenga, 0727, South Africa

E-mail: phalamasoga@gmail.com

Abstract. The increasing demand for high energy density rechargeable batteries has fuelled the interest in the research, development and manufacturing of new battery systems capable of powering high powered machinery as well as rechargeable household appliances. Pyrolusite (β-MnO_2) is the most stable and abundant polymorph of manganese dioxide and a potential cathode material for rechargeable lithium-ion batteries. In this study, a combination of evolutionary algorithm techniques and density functional theory methods are employed to determine the stabilities of MnO_2 nanoclusters across the energy landscape. We investigate the energetics and structural configurations for $(MnO_2)n=1-6$ nanoclusters. The most stable nanoclusters are made of a cubic structure consisting of two manganese and two oxygen atoms for various cluster sizes. The stable structures tend to migrate to more circular compact configurations after geometry optimization using density functional theory. As the temperature is increased from 200K to 1300K, the change in the bond angles and bond distances is measured. An increment of the exterior angles and bonding lengths along with the decrease of the interior angles is observed further emphasizing the migration to a more circular compact configuration.

1. Introduction

The growing demand for energy has caused an increase in scientific research focusing on renewable and rechargeable energy supplies as a way of supplementing the pressure on the rapidly declining fossil fuel reserves. The dependence on fossil fuels as the main source of energy for powering the industrial revolution has contributed considerable damage to the environment [1]. Recent developments in the field of scientific research on energy storage has already begun producing results as evident in the production of electric vehicles (EVs) and hybrid electric vehicles (HEVs) [2]. Among all types of secondary batteries, lithium-ion batteries have attracted the most attention as they are characterized by high energy density and high power density [3]. One of the challenges for improving the performance of lithium-ion batteries to meet increasingly demanding requirements for energy storage is the development of suitable cathode materials [4]

Pyrolusite (β-MnO_2) is regarded as the most stable and abundant polymorph of manganese dioxide. It crystallizes into the rutile crystal structure with three-coordinate oxide and octahedral metal centers. Nanostructuring has been shown to improve the performance of energy storage materials although the mechanisms for this improvement are not fully understood on the atomic-scale. Several nanostructured MnO_2, including nano-crystals of different shapes; nanowires, nanotubes, nanoclusters and nanobelts, have been synthesized and can be used as new materials for battery systems [5, 6]. Experimentally, nanoscaling of cathode materials is still a challenge due to complexities associated with the synthesis and monitoring of reactions occurring at the nanoscale. MnO_2 structures have been simulated and

studied in varying shapes and architectures, that is, nanosheet, nanorod and mesoporous [7]. Consequently, recent advances in computational resources provide options in simulating materials at the nanoscale, thereby shedding light and reducing costs on this very important field of research [8, 9]. In this paper, structural configuration and stability of MnO_2 nanoclusters are investigated using density functional theory, as an approach of refining nanocluster models developed using interatomic potentials. Also the effect of temperature change on nanocluster configuration is investigated.

2. Methodology

Evolutionary algorithms (EA) have been used previously to determine the local minima of desired atomic structures and produced better results compared to other methods [7, 10]. The fundamental idea behind evolutionary algorithms is performing a process that simulates natural selection through survival of the fittest [11, 12]. The method avoids many problems associated with a single starting point by setting up a population of candidate clusters, hence the end product of each EA cycle is a new population of candidate structures [13]. Evolutionary algorithm techniques were used previously to investigate the stability of $(MnO_2)_n$ n=1-4 [14] and a more detailed methodology is presented therein. The multistage configurations procedure for determining the low-energy configurations for MnO_2 clusters is used. In the first EA cycle the candidate structures are configurations in which the ionic coordinates are randomized. In stages 1 and 2, EA make use of the local optimization routines within the GULP program [15] based on Interatomic Potential (IP) method, to relax all newly created structures through breeding or randomization. In stages 3 and 4 of the EA cycle, the better clusters within the final population, as measured by the energy of formation, are selected for analysis or further refinement using a density functional theory (DFT) method.

A multistage procedure is implemented in order to predict the low-energy configurations for neutral, stoichiometric small clusters of MnO_2. For each cluster, n=1 to 6 in the first stage, low-energy stationary points are found on the three different energy hypersurfaces that are defined by interatomic potentials. In EA simulations, the ground-state configuration for a cluster with predefined composition becomes a plausible candidate. In this paper, the all electron density functional theory method with a local numerical orbitals basis set and local optimization techniques as implemented in the CASTEP [16] code were employed to further investigate MnO_2 nanocluster stability trend and temperature effects. Thus, the lowest energy candidate structures, as measured by the energy of formation using the interatomic potential method were subjected to geometry optimization using GGA-PBEsol (stages 3 to 5). The planewave basis set energy cut-off was set at 500 eV. For atomic positions to be considered fully relaxed, the convergence parameters were set as follows: total energy tolerance 1×10^{-6} eV/atom, maximum force tolerance 0.05 eV/nm and maximum stress component 0.1 GPa. The stable nanoclusters were placed centrally in a 10 x 10 x 10 Å crystal box, large enough to ensure that there were no interactions between the system and its self-image along all the axes within the periodic boundary conditions.

3. Results and Discussions

Geometrical configurations of $(MnO_2)_{n=1-6}$ nanoclusters and their order of stability as determined by the density functional theory are presented. Thus, the structural properties based on atomic configurations as determined by bond lengths and bond angles are discussed along with stability of the nanoclusters. In Figure 1, the most stable nanocluster for each cluster size as measured by formation energy is presented together with bond lengths after optimization. A small letter labels the nanocluster with a number indicating the number of atoms (n), followed by dashed number indicating the stable local minima structures as determined by the evolutionary algorithms sequence (e.g. n1-2). The bond lengths between the atoms in the nanoclusters were measured.
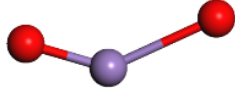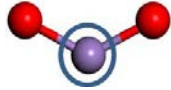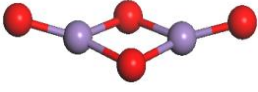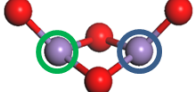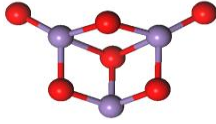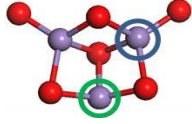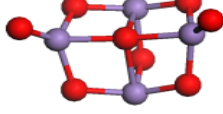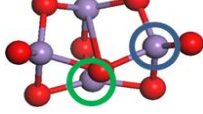
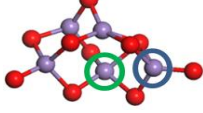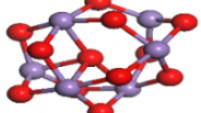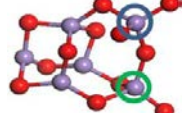| Structure $(MnO_2)_{n=1}$	Interatomic potentials (IP) method [17]	Density Functional Theory (DFT) method	DFT Bond Length (Å)
n1-2			Mn1-O1=1.655 Mn1-O2=1.655
n2-2			Mn1-O1=1.652 Mn1-O2=1.801 Mn1-O3=1.802 Mn2-O4=1.651
n3-2			Mn1-O1=1.661 Mn1-O2=1.864 Mn1-O3=1.828 Mn2-O2=1.771
n4-1			Mn1-O1=1.652 Mn1-O2=1.805 Mn1-O3=1.816 Mn2-O2=1.833
n5-1			Mn1-O1=1.649 Mn1-O2=1.773 Mn1-O3=1.848 Mn2-O2=1.905
n6-2			Mn1-O1=1.694 Mn2-O2=1.808 Mn1-O3=1.815 Mn2-O2=1.839

Figure 1: Atomic configurations and bond lengths for $(MnO_2)_{n=1-6}$ nanocluster as predicted by IP (before optimization) and DFT (after optimization) methods.

The interatomic interactions between the manganese and oxygen atoms are classified as follows: Mn1 is encircled in blue while Mn2 is encircled in green. The oxygen atoms are numbered 1, 2, 3, 4 … with O1 being the first oxygen from the right hand side, followed by O2 as the second oxygen from the right side bonded to Mn1 or Mn2. The same identification was used for O3 and O4. There is a notable decrease in bond length and bond angles of all the nanoclusters after geometry optimization with density functional theory method. The change in bond parameters suggests that the configuration for the nanocluster becomes compact. DFT predicts the bond lengths ranging between 1.655 Å and 1.905 Å for $(MnO_2)_{n=1-6}$. For n = 1, 2, 3 and 6 the second most stable structures as measured and predicted by interatomic potentials are found to be the most stable structures and this is in agreement with previous studies where a different DFT code, FHI-AIMS was used by Maphanga et al. [17] to refine IP nanocluster structures. On the other hand, n=4 and 5 predict the same nanocluster structures as those predicted by interatomic potentials to be the most stable. DFT predicts the atomic arrangement of the local minima structures to be bending to form a quasi-like isomer for all the systems.

It is evident from the density functional theory techniques that compact ring structures consisting of a cubic structure for the orientation of the two manganese and two oxygen atoms is the most stable and preferred orientation, which correlates with previous studies [9, 18]. Furthermore, experimental photoelectron spectroscopy (PES) studies of isostructural titanium dioxide (TiO_2) nanoclusters by Zhai et al. [19] reported that compact ring structures are the most stable. The predicted most stable MnO_2 nanoclusters have identical bonds between the manganese and oxygen atoms but slightly different bond angles between the manganese and two oxygen atoms for n=1 to n=4. Similar trends have been reported for the isostructural TiO_2 by Hamad [9]. Furthermore, most stable structures adopting compact ring

configurations are in agreement with findings by Woodley et al. [20, 21], which suggested that the smallest clusters preferred shorter average bond distances as opposed to a higher average coordination of the constituent atoms. Thus, nanoclusters prefer compact ring configuration than a linear atomic arrangement. The Mn-O bond lengths decrease slightly after optimization with DFT and the bond angles for the atoms at the outer side (angles at both sides of the Mn1 and Mn2 atoms encircled in blue and green respectively) also decrease. The DFT method predicts a configuration with two-terminal Mn-O bonds. The complexity of the energy landscape increased with the increase in cluster size as seen with the n5-1 and n6-2 nanoclusters where the atoms formed several different bonds after optimization.
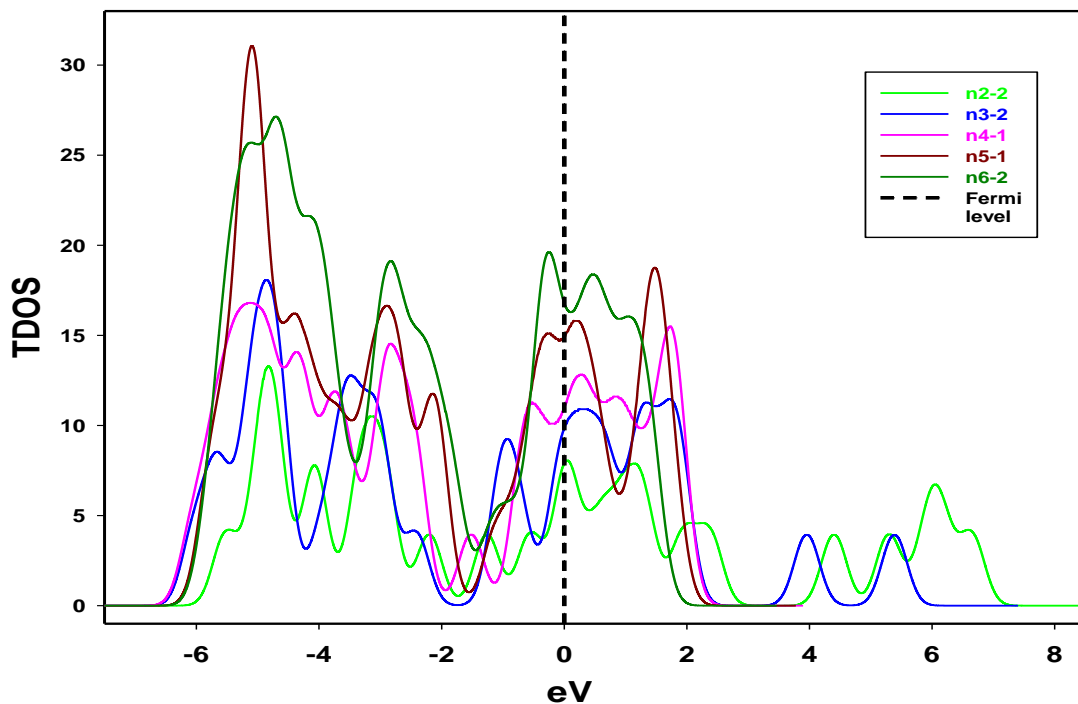

Figure 2: Total density of states for the most stable nanoclusters $(MnO_2)_{n=2-6}$

Figure 2 shows the total density of states (TDOS) of the five most stable nanoclusters excluding the smallest n1-2 nanocluster with the fewest atoms as compared to the other nanoclusters. From the graph, we observe that as the size of the cluster is increasing, contributions at the Fermi level are also increasing. This is expected as the nanocluster stability increases with the cluster size. It is also observed that the highest peaks on both sides of the Fermi level are moving further away from the Fermi level as the cluster size is increased which shows the varying metallic behavior of the nanoclusters. The density of states for the different stable nanoclusters depict same behaviour; with slight differences on individual atomic contributions due to different coordination numbers and bond lengths for various nanoclusters. Thus, the nanoclusters are predicted to be metallic with the density of states showing no band gap at the Fermi level at ambient pressure. The hybridization of the protruding peaks from the individual atoms leads to the presence of the high peaks on the total DOS. The hybridization of the Mn 3d orbital and the O 2p orbital forming a covalent bond, is mainly due to manganese contributing the majority DOS as it is more reactive and less stable. The highest peak on the valence band corresponds to the n5-1 contributions and is also referred to as the valence band maximum.

Lastly, the effect of temperature on stability of the nanoclusters was investigated using an *ab-initio* molecular dynamics approach. The NVE ensemble using the GGA-PBE functionality in CASTEP was used to determine the effect of temperature change on the nanoclusters. For illustrative purposes, the temperature dependence results for n5-1 nanocluster are presented and shown in Figure 3. It is noted from the graph that, there is a linear increase from 200 K to 500 K. The total energy drops at 600 K,

followed by another linear increase up to 900 K. The nanocluster shows two possible phase transitions at approximately 500 K and 1000 K. As it was observed with the other nanoclusters discussed above, the system is less stable at higher temperatures. The O-Mn-O α angle increases at most temperatures except at 600 K and 900 K, which are the temperatures where phase transitions are observed. Analysis of Mn-O bond lengths revealed a slight change for all the nanoclusters, with the bond lengths ranging from 1.635 Å to 1.949 Å. The experimental melting point of bulk pyrolusite was recorded to be 808 K (535 ºC) [22]. The nanoclusters tend to be stable at lower temperatures while depicting a higher disorder at higher temperatures.
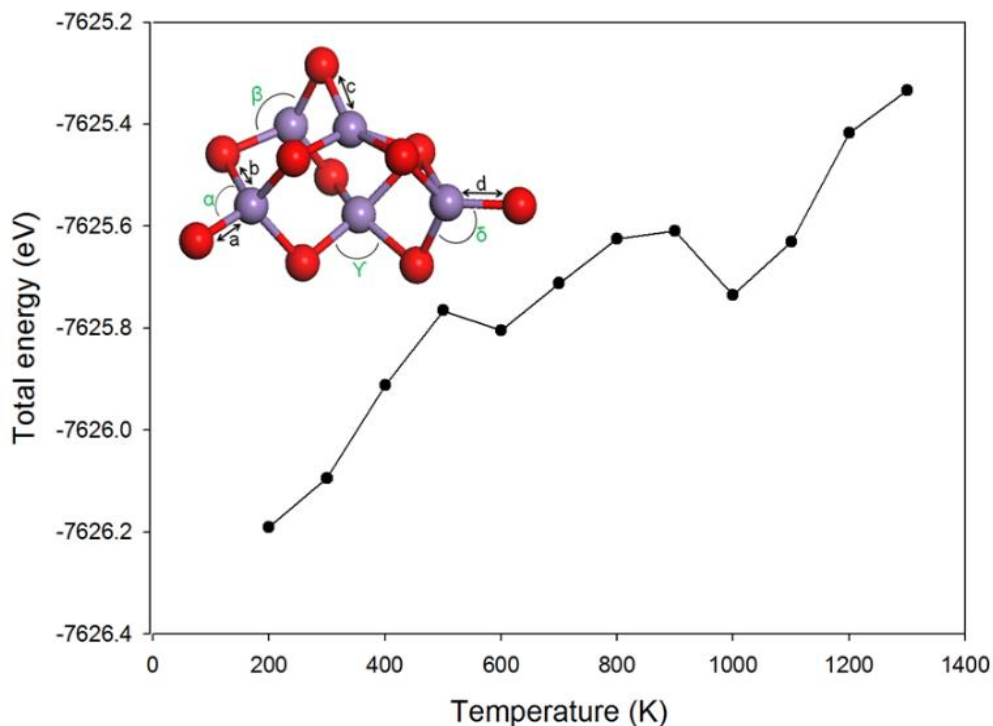

Figure 3: Total energy versus temperature graph for the n5-1 nanocluster.

The stability at low temperatures indicates that there is minimal atomic movement when the temperature is low, hence minimal entropy of the system. The average stable temperature for simulated nanoclusters was calculated to be 300K (26.85 ºC). This stable temperature is good as most commercial lithium-ion batteries based on bulk systems show good performance at room temperature 298 K and 333 K.

4. Conclusion

The electronic structure methods were employed successfully to validate the order of stability for previously generated MnO_2 nanoclusters. The plausible nanocluster structures from interatomic potential simulations were refined using density functional theory technique because interatomic potentials are parameterized with reference to bulk crystalline properties and may cause difficulties when applied to clusters where the coordination number and bonding may differ. The most stable nanoclusters are in agreement with those that have been reported previously using FHI-AIMS code, particularly for $(MnO_2)_n$ n= 1-4. Analyzing the basic configurations of the stable nanoclusters, compact ring structures consisting of a cubic structure with two manganese and two oxygen atoms dominate the make-up of the most stable structures. The nanoclusters preferred shorter average bond distances as opposed to a higher average coordination of the constituent atoms. Larger sized structures adopted bubble structures and the bond lengths increased with cation size. The linear configuration was found

to be less favorable for the systems, which explains the migration to a circular compact configuration in the stable MnO_2 nanoclusters. The average stable temperature for the simulated nanoclusters was calculated to be 300K (26.85 ºC) which indicated minimal atomic movements at low temperatures.

References
[1] Hook M and Tang X 2012 *Energy Policy.* **52** 797
[2] Yamada A, Chung S C and Hinokuma K 2001 J. Electrochem. Soc. **148** 224
[3] Languang L, Xuebing H, Jianqiu L, Jianfeng H and Minggao O 2013 *J. Power Sources.* **226** 272
[4] Fergus J W 2009 *J. Power Sources.* **195** 939
[5] Balachanran D, Morgan D and Ceder G 2002 *J. Solid State Chem.* **166**, 91
[6] Hu CC and Tsou TW 2002 *Electrochimica Acta,* **47,** 3523
[7] Sayle T X T, Maphanga R R, Ngoepe P E and Sayle D C 2009 *J. Am. Chem. Soc.* **131** 6161
[8] Tompsett D A, Parker S C and Islam M S 2014 *J. Am. Chem. Soc.* **136** 1418
[9] Hamad S, Catlow C R A, Woodley S M, Lago S and Mejias J A 2005 *J. Phys. Chem. B.* **109** 15741
[10] Sugantha M, Ramakrishnan P A, Hermann A M, Warmsingh C P and Ginley D S 2003 *Int. J. Hydrogen Energy.* **28** 597
[11] Zheng-Jun P 1998 Evolutionary Algorithm. *Tsinghua University Press, Beijing*
[12] Holland J H 1992 *Sci. Amer.* **66**
[13] Lian-Jun L 2000 *Int. J. Mod. Phys. C.* **11** 183
[14] Ngoepe P E, Maphanga R R and Sayle D C 2013 Chapter 9, John Wiley and Sons, LTD, UK
[15] Gale J D 1997 J. Chem. Soc. **93** 629
[16] Clark S J, Segall M D, Pickard C J, Hasnip P J, Probert M I J, Refson K and Payne M C 2005 Z. *Kristallogr.* **220** 567
[17] Maphanga R R, Ngoepe P E, Catlow C R A and Woodley S M 2015 *South African Institute of Physics Conference Proceedings*
[18] Nagarajan V, Saravanakannan R and Chandiramouli 2014 *Int. J. Chem. Tech. Res.* **6** 2962
[19] Zhai H and Wang L 2007 *J. Am. Chem. Soc.* **129** 3022
[20] Woodley S M 2011 *Proc. R. Soc. A: Math. Phys. Eng. Sci.* **467** 2020
[21] Woodley S M 2013 *J. Phys. Chem. C.* **117** 24003
[22] ChemSpider. Royal Society of Chemsitry. Manganese dioxide [Online] Available: http://www.chemspider.com/Chemical-Structure.14117.html# [Accessed 21/11/2017]